Establishing a benchmark for comparative analysis of thin and thick plate modal frequencies: A non-dimensional paradigm

Conference Paper · August 2024

CITATIONS
0

READS
89

3 authors:

Sebastian Duran
University of Bologna
17 PUBLICATIONS **15** CITATIONS
SEE PROFILE

Henna Tahvanainen
University of Bologna
31 PUBLICATIONS **86** CITATIONS
SEE PROFILE

Michele Ducceschi
University of Bologna
75 PUBLICATIONS **448** CITATIONS
SEE PROFILE

25-29 August 2024
inter.noise
NANTES FRANCE

Establishing a benchmark for comparative analysis of thin and thick plate modal frequencies: A non-dimensional paradigm

Sebastian Duran[1]
DIN, University of Bologna
Viale del Risorgimento 2, 40136, Bologna, Italy

Henna Tahvanainen[2]
DIN, University of Bologna
Viale del Risorgimento 2, 40136, Bologna, Italy

Michele Ducceschi[3]
DIN, University of Bologna
Viale del Risorgimento 2, 40136, Bologna, Italy

ABSTRACT

This study presents a methodological framework to establish a standardised baseline for comparing the vibrational characteristics of thin and thick rectangular orthotropic plates in acoustics. The research addresses the inherent difficulties associated with varying plate parameters by proposing the use of non-dimensional frequencies for comparative assessments. It will be shown that, under the thin-plate approximation, plates with identical aspect ratios, boundary conditions, and elastic constant ratios exhibit identical non-dimensional modal frequencies and shapes. The proposed methodology involves generating baseline non-dimensional frequencies and modal shapes via numerical simulations for a reference plate with specified parameters. Subsequent analysis entails systematically varying plate thickness while monitoring deviations of non-dimensional frequencies from the baseline. This process finally allows to determine up to which mode number the discrepancy in the dimensionless frequency between the baseline and the ensuing modelled plates can be confined within certain tolerance values. Notably, the comparison is conducted on an eigenshape basis, thereby circumventing the consideration of dimensional frequencies. This approach offers a structured framework for comparative analysis, centred on identifying modes exhibiting thin behaviour regardless of dimensional frequencies, stressing the objectivity of the presented methodology.

1. INTRODUCTION

Plates are structural elements found across various domains and disciplines, and musical acoustics is no exception. Most acoustic stringed instruments can radiate sound efficiently thanks

[1]sebastian.duran2@unibo.it

[2]henna.tahvanainen@unibo.it

[3]michele.ducceschi@unibo.it

to a plate-like structure. Examples abound, from keyboard instruments such as the harpsichord and the piano presenting large soundboards, to guitar-like instruments including a back and a top plate and bowed string instruments with arched plates. In these cases, the plates are almost exclusively built from tonewoods, inheriting an orthotropic property along the three main axes of tree logs: radial, longitudinal and tangential [1]. The design process of the string instrument deals with wood's material properties and the soundboard's geometric properties, both of which shape the instrument's tone. Designing soundboards and plates to satisfy the desired acoustical and musical targets is, thus, a fundamental problem in instrument making, and it can be aided by modelling.

The mathematical models for the plates fall into two main categories: thin-plate and thick-plate models [2]. Usually, a thin-plate model can be derived from a more general thick-plate model when the thickness becomes small. This is true for the Kirchhoff-Love thin plate model, a special case of the more general model by Mindlin and Reissner [3, page 486]. The former is still preferred in many cases because it is more easily understood, its dispersion relation is easily derived, and it is more easily implemented in simulation. This preference is clear in musical acoustics, where plates and soundboards are commonly described as being "thin" [4–7]. Whilst this is a convenient idealisation, thin and thick are frequency-dependent qualities: a thin-plate model may do well in describing the behaviour of a plate in the lower frequency range and fail spectacularly in the mid-to-high range.

Computing the dispersion relations of the two models using the available model parameters for a given plate is one way of assessing the models' mutual deviation in the frequency domain [2, 8]. This method, however, neglects the role of the surface area and boundary conditions in yielding the modal frequencies, which ultimately determine the acoustics of the plate. Clearly, the size of the plate matters in determining the frequency range where the thin approximation holds. Piano soundboards up to eight millimetres thick, for example, may be considered "thin", but guitar top boards would seldom be thicker than two or three millimetres. Some authors have identified length-to-thickness ratios, which may be used as practical advice for the analysis of plate vibration. For instance, in [9], eight is given as a lower bound for such a ratio, below which the thick-plate effects cannot be neglected. It may then be useful to incorporate the role of the surface area to assess the model's deviation within the modal domain: this work explores such a possibility through dimensional analysis. It will be shown that, in the thin-plate approximation, plates presenting the same boundary conditions, aspect ratio and elastic constant ratios also present the same non-dimensional frequencies and modal shapes when the non-dimensionalisation is performed according to the geometric parameters such as the thickness and the surface area. Various case studies are shown for plates differing in size and thickness. This approach offers a structured framework for comparative analysis, centred on identifying modes exhibiting thin behaviour regardless of dimensional frequencies.

2. THEORETICAL BACKGROUND

The vibration of an orthotropic plate can be described via the Mindlin-Reissner model. This is a system of three equations describing the time evolution of the flexural displacement and two shear angles. Let the flexural displacement be $u = u(\mathbf{x}, t) : \mathcal{V} \times \mathbb{R}_0^+$ and the shear angles be $\Psi = \Psi_\circ(\mathbf{x}, t) : \mathcal{V} \times \mathbb{R}_0^+$ where $\circ$ may denote either x or y. Here, $\mathbf{x} \in \mathcal{V} \subseteq \mathbb{R}^2$ are the spatial coordinates, and $\mathcal{V}$ is the domain of definition, left unspecified for the moment. Here, and in what follows, x denotes the longitudinal orthotropic direction, y is radial, and z is tangential. In quarter-sawing, z is the

direction along the thickness of the board. With this notation, the system reads [2]:

$$\frac{\rho h^3}{12}\partial_t^2\Psi_x = D_1\partial_x^2\Psi_x + \frac{D_4}{4}\partial_y^2\Psi_x + \left(\frac{D_2}{2}+\frac{D_4}{4}\right)\partial_x\partial_y\Psi_y - \kappa^2 G_{xz} h\,(\Psi_x + \partial_x w)\,, \tag{1a}$$

$$\frac{\rho h^3}{12}\partial_t^2\Psi_y = D_3\partial_y^2\Psi_y + \frac{D_4}{4}\partial_x^2\Psi_y + \left(\frac{D_2}{2}+\frac{D_4}{4}\right)\partial_x\partial_y\Psi_x - \kappa^2 G_{yz} h\left(\Psi_y + \partial_y w\right)\,, \tag{1b}$$

$$\rho h\partial_t^2 w = \kappa^2 G_{xz} h\partial_x(\Psi_x + \partial_x w) + \kappa^2 G_{yz} h\partial_y(\Psi_y + \partial_x w)\,. \tag{1c}$$

The model depends on four rigidity constants, denoted by $D_\circ$, two shear moduli $G_\circ$, the shear correction factor $\kappa \approx 0.9$, the thickness of the plate h, assumed constant throughout $\mathcal{V}$, and the volume density ρ. The rigidity constants are defined in terms of the Young's moduli as follows:

$$D_1 := \frac{E_x h^3}{12(1-\nu_{xy}\nu_{yx})},\; D_3 := \frac{E_y h^3}{12(1-\nu_{xy}\nu_{yx})},\; D_4 := \frac{G_{xy} h^3}{3},\; D_2 := \frac{\nu_{yx} E_x h^3}{6(1-\nu_{xy}\nu_{yx})}. \tag{2}$$

Note that, because of the symmetry in the compliance matrix, $\nu_{yx}E_x = \nu_{xy}E_y$, and hence one out of two Poisson's ratios is fixed through this relation. Lower-order theories may be derived by simplifying Mindlin-Reissner model (Eq. 1). In the thin-plate approximation, the inertia terms of the cross sections are neglected, and furthermore, the cross sections are assumed to remain normal to the plate's central lines, leading to $\Psi_\circ = -\partial_\circ w$, where $\circ$ is either x or y. Thus, using these approximations, Equation 1a and Equation 1b can be substituted in Equation 1c, which becomes the Kirchhoff-Love equation:

$$\rho h\partial_t^2 w = -D_1\partial_x^4 w - (D_2+D_4)\partial_y^2\partial_x^2 w - D_3\partial_y^4 w. \tag{3}$$

2.1. Dispersion Relations

Computing the dispersion relations of Eq. 1 and Eq. 3 is one common way of assessing the reliability of the thin-plate approximation for a given plate. Dispersion relations assume that the plates are defined on an unbounded domain, such that $\mathcal{V} = \mathbb{R}^2$ for this analysis. For the Mindlin-Reissner model, the dispersion relation is obtained by substituting a test solution of the form:

$$\mathbf{u} := \begin{bmatrix}\Psi_x\\ \Psi_y\\ w\end{bmatrix} = \begin{bmatrix}\hat{\Psi}_x\\ \hat{\Psi}_y\\ \hat{w}\end{bmatrix} e^{j(\omega t + \mathbf{k}\cdot\mathbf{x})} := \hat{\mathbf{u}} e^{j(\omega t+\mathbf{k}\cdot\mathbf{x})} \tag{4}$$

in Eq. 1. Here, the "hat" variables are (generally complex) constant amplitudes. The vector $\mathbf{k} := [k_x, k_y]^\top$ denotes the vector of wavenumbers along x and y. Substituting this expression, one gets:

$$\left(\mathbf{K}(k_x,k_y) - \omega^2\mathbf{M}\right)\hat{\mathbf{u}} = 0, \tag{5}$$

for appropriate mass and stiffness matrices $\mathbf{M}, \mathbf{K}$, not given here for brevity. The matrices are 3×3, so the dispersion relation presents three branches corresponding to the three eigenvalues of the equation above. The three eigenvalues may be labelled $\omega^2_{\hat{w}}, \omega^2_{\hat{\Psi}_x}, \omega^2_{\hat{\Psi}_y}$ as, at low wavenumbers, their behaviour is mostly dominated by the corresponding dynamic variable. Although all three dynamic variables contribute to each branch, this is a convenient labelling system. For the Kirchhoff-Love model, the dispersion relation is obtained analogously as:

$$\omega^2\rho h\hat{w} = (D_1 k_x^4 + D_3 k_y^4 + (D_2+D_4)k_x^2 k_y^2)\,\hat{w}. \tag{6}$$

The dispersion relations for the two models are shown and compared in Figure 1, for plates of increasing thickness. The top row shows the three branches of the Mindlin-Reissner dispersion

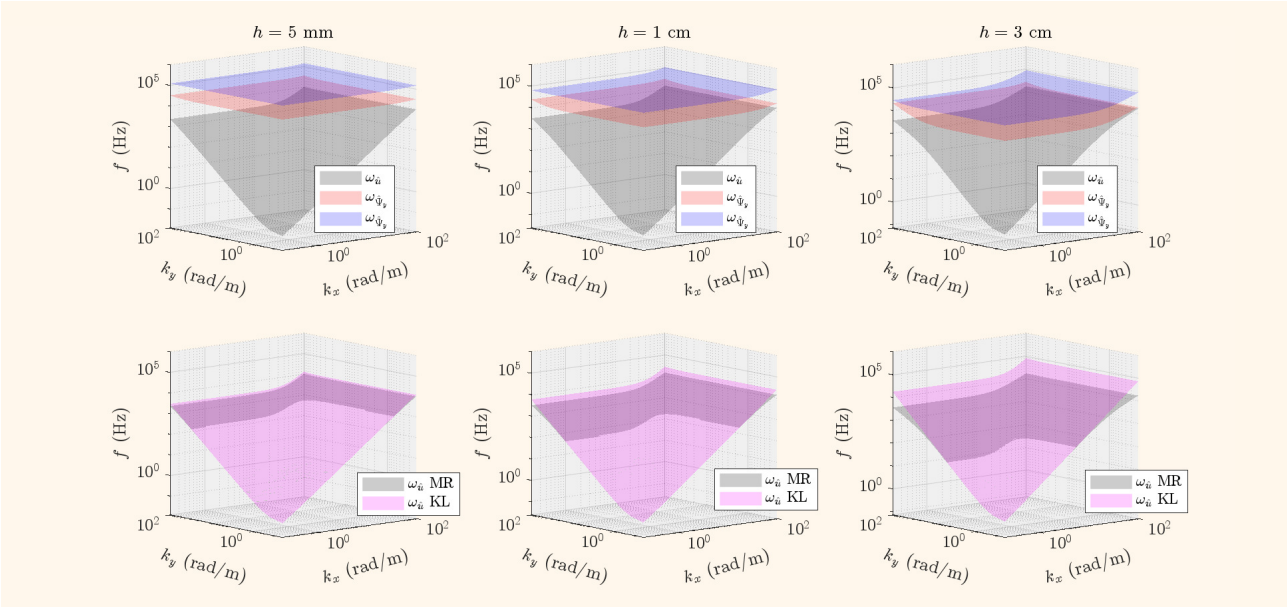

Figure 1: Dispersion relations. Top row: the three branches of the Mindlin-Reissner dispersion relation, as per Equation 5. Bottom: The lower branch of the Mindlin-Reissner (grey) against the Kirchhoff-Love dispersion relation (magenta). The plate elastic constants are typical spruce parameters, as found in [10, page 96].

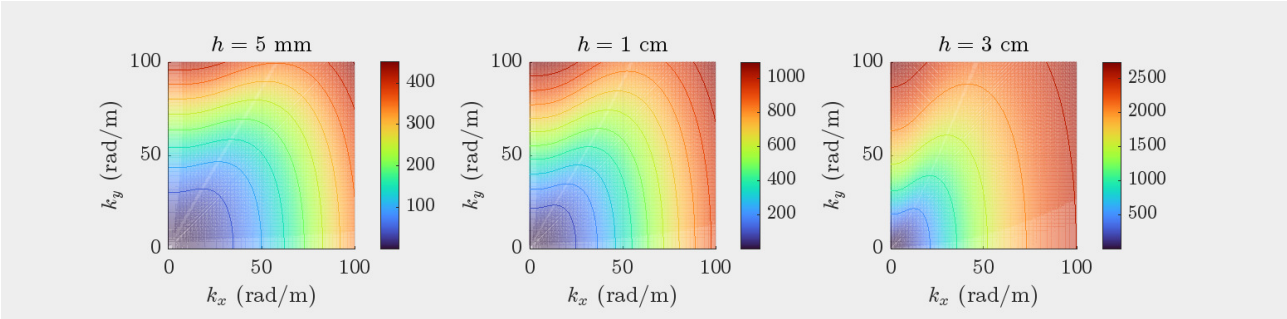

Figure 2: Cent deviations, including contour lines, between the lower branch of the Mindlin-Reissner dispersion relation and the Kirchhoff-Love dispersion relation, as a function of the wavenumbers k_x, k_y. The same plates as per Figure 1 are considered. The deviations are defined as $\Delta_{cent}\omega := 1200\log_2(\omega_{KL}/\omega_{MR})$. A deviation of 100 cents corresponds to one semitone.

relation. One distinctive feature is the presence of non-zero lower bounds for two branches: these bounds are "cutoff" frequencies analogous to the cutoff frequency observed in the Timoshenko beam [11, 12]. They can be interpreted as frequencies below which the shear angle effects are minimal. They are recovered by computing the limit of the dispersion relation for vanishing k_x, k_y, and are:

$$\omega_{0x} := h^{-1}\sqrt{12\kappa^2 G_{xz}\rho^{-1}}, \quad \omega_{0y} := h^{-1}\sqrt{12\kappa^2 G_{yz}\rho^{-1}}. \tag{7}$$

These expressions are inversely proportional to the thickness, meaning that, as h increases, they become increasingly smaller, enhancing the thick-plate effects at progressively lower frequencies. When the thickness is $h = 5$ mm, for typical tonewood elastic constants (see e.g. [10, page 96]), such cutoff frequencies are found well above 10 kHz. Comparing the lower branch of the Mindlin-Reissner dispersion relation against the dispersion relation of Kirchhoff-Love, some noticeable differences take place for moderately thick plates ($h = 1$ cm) for frequencies well within the audible range. Such differences become evident at even lower frequencies for thicker plates ($h = 3$ cm), though such large thicknesses are never found in musical instrument plates and soundboards. The

cent deviation between the frequencies of the lower branch of the Mindlin-Reissner dispersion relation against Kirchhoff-Love is offered in Figure 2, as a function of the wavenumbers k_x, k_y. When $h = 5$ mm, differences of at least one semitone are observed for relatively low wavenumbers ($k_\circ \approx 30$).

As explained above, dispersion analysis is carried out assuming an unbounded domain. In reality, a quantisation of the wavenumbers and corresponding frequencies takes place when boundary conditions are imposed at the plate's edges, yielding the modes of the system. A mode's wavenumber along x and y depends on the respective length along the same direction such that deviations from the thin-plate model may occur earlier or later in the modal sequence, according to the plate's size. The following analysis addresses such differences in the modal domain.

2.2. Non-dimensional model

In what follows, assume a bounded rectangular domain $\mathcal{V} := [0, L_x] \times [0, L_y]$, where L_x, L_y are the plate's edge lengths. In order to assess the deviation of a plate's modes from the corresponding thin-plate modal basis, it is necessary to rescale the modal frequencies according to useful scaling parameters. The idea is to group plates into families sharing the same modal frequencies under scaling, forming an invariant set. Such a set may be obtained immediately through non-dimensionalisation of the Kirchhoff-Love model, Equation 3. To that end, collect D_4 on the right-hand side of Equation 3, and divide both sides by ρh. One gets:

$$\partial_t^2 u = -\gamma^2 \left((\partial_x^4 + \nu_{yx} \partial_x^2 \partial_y^2) p + (\partial_y^4 + \nu_{xy} \partial_x^2 \partial_y^2) q + \partial_x^2 \partial_y^2 \right) u, \tag{8}$$

where $\gamma^2 := \rho^{-1} h^{-1} D_4$, and $p := D_4^{-1} D_1$, $q := D_4^{-1} D_3$. Following the derivation in [13], non-dimensionalization proceeds as follows. Define:

$$u = A^{\frac{1}{2}} \bar{u}, \quad x = A^{\frac{1}{2}} \bar{x}, \quad y = A^{\frac{1}{2}} \bar{y}, \quad t = \gamma^{-1} A \bar{t}, \tag{9}$$

where the overbar indicates non-dimensional variables, and $A := L_x L_y$ is the plate's area. Consequently, Equation 8 transforms into:

$$\partial_{\bar{t}}^2 \bar{u} = -\left((\partial_{\bar{x}}^4 + \nu_{yx} \partial_{\bar{x}}^2 \partial_{\bar{y}}^2) p + (\partial_{\bar{y}}^4 + \nu_{xy} \partial_{\bar{x}}^2 \partial_{\bar{y}}^2) q + \partial_{\bar{x}}^2 \partial_{\bar{y}}^2 \right) \bar{u}, \tag{10}$$

over the non-dimensional space $\bar{\mathcal{V}} = (\bar{x}, \bar{y}), |, 0 \le \bar{x} \le \sigma^{\frac{1}{2}}, , 0 \le \bar{y} \le \sigma^{-\frac{1}{2}}$, where $\sigma := L_y^{-1} L_x$ denotes the aspect ratio. Transforming Equation 10 into the frequency domain (with $\partial_{\bar{t}} \to j\bar{\omega}$, $\partial_{\bar{x}} \to j\bar{k}_{\bar{x}}$, $\partial_{\bar{y}} \to j\bar{k}_{\bar{y}}$) yields the non-dimensional dispersion relationship:

$$\bar{\omega}^2 = (\bar{k}_{\bar{x}}^4 + \nu_{yx} \bar{k}_{\bar{x}}^2 \bar{k}_{\bar{y}}^2) p + (\bar{k}_{\bar{y}}^4 + \nu_{xy} \bar{k}_{\bar{x}}^2 \bar{k}_{\bar{y}}^2) q + \bar{k}_{\bar{x}}^2 \bar{k}_{\bar{y}}^2, \tag{11}$$

from which we can deduce the modal frequencies $\bar{\omega}_{m,n}$, as a quantized form of Equation 11. Here, $m, n \in \mathbb{N}$ denote a pair of modal indices related to the nodal lines in the x and y directions. For fixed p, q, the quantisation depends exclusively on the boundary conditions $\mathscr{B}$ and the aspect ratio σ. Thus, the non-dimensional frequencies can be expressed as:

$$\bar{\omega}_{m,n}^2 = a_{m,n} p + b_{m,n} q + c_{m,n}, \tag{12}$$

for modal-dependent parameters a, b, c, depending exclusively on $\mathscr{B}$ and σ [13].

The scaling suggested in Equation 10 bears important interpretative results. Assuming constant material parameters (density and elastic constants), the scaling depends exclusively on the thickness h and the surface area. Thus, the deviation of a plate's modal frequencies and shapes from the reference baseline can be tracked as a function of h and A. Since scaling laws are more conveniently used in this work, it is useful to define a non-dimensional parameter, defined

in terms of h and A. When the aspect ratio is constant, consider the following non-dimensional parameter:

$$\eta := \sqrt{A/\sigma}\, h^{-1} = L_x h^{-1}. \tag{13}$$

This thickness-to-length parameter has been used to quantify useful ranges of validity of the thin-plate theory. In [9], such a range is given as:

$$8 \leq \eta \leq 80. \tag{14}$$

3. METHODS

The analysis presented above derived an expression for the baseline modal frequencies in the limit of small thickness (Eq. 12). The existence of such a baseline sequence of modes will be tested below for a family of plates. In what follows, four plates are considered. The plates share the same aspect ratio $\sigma = 3$, but present decreasing surface areas A. The geometric parameters are summarised in Table 1.

	Plate 1	Plate 2	Plate 3	Plate 4
L_x (m)	3.6	1.2	0.6	0.24
L_y (m)	1.2	0.4	0.2	0.08
A (m^2)	4.32	0.48	0.12	0.0192

Table 1: Geometric parameters of the plates considered in this analysis. For all plates, the thickness values are selected as $h = 0.5, 1, 5, 10, 20, 30$ mm. To compute the baseline, a thickness of $h = 0.1$ mm is selected. Note that the plates share the same aspect ratio $\sigma = 3$.

ρ	E_x	E_y	E_z	G_{xy}	G_{xz}	G_{yz}	ν_{xy}	ν_{xz}	ν_{yz}
390	10.9	0.64	0.42	0.58	0.59	0.026	0.39	0.49	0.64
kg / m^3	GPa	GPa	GPa	GPa	GPa	GPa			

Table 2: Input COMSOL elastic constants, inspired by the table in [10, page 96] for spruce.

The material parameters are the same for the four plates, summarised in Table 2. Note that these will be used as input parameters for the COMSOL simulations in the thin plate interface and, hence, include E_z, ν_{xz} and ν_{yz} although these do not appear explicitly in Eq. 1. These are reference spruce parameters inspired by the table in [10, page 96].

According to the scaling in Eq. 10, the scaled modal frequencies are obtained as:

$$\bar{\omega}^2_{m,n} := D_4^{-1}\, \rho h A^2\, \omega^2_{m,n}. \tag{15}$$

Deviations of the results from the baseline can take three forms: distortion of the modal shape, modal crossings, and change of modal frequency. The Modal Assurance Criterion (MAC) can quantify the first two. For two column modal shape vectors $\mathbf{U}, \mathbf{U}'$ of two modes, the MAC index is a scalar value defined as [14]:

$$\mathrm{MAC}(\mathbf{U}, \mathbf{U}') := \frac{|\mathbf{U}^\top \mathbf{U}'|^2}{\|\mathbf{U}\|^2\, \|\mathbf{U}'\|^2}. \tag{16}$$

Values close to one indicate that the modal shapes $\mathbf{U}, \mathbf{U}'$ are highly correlated.

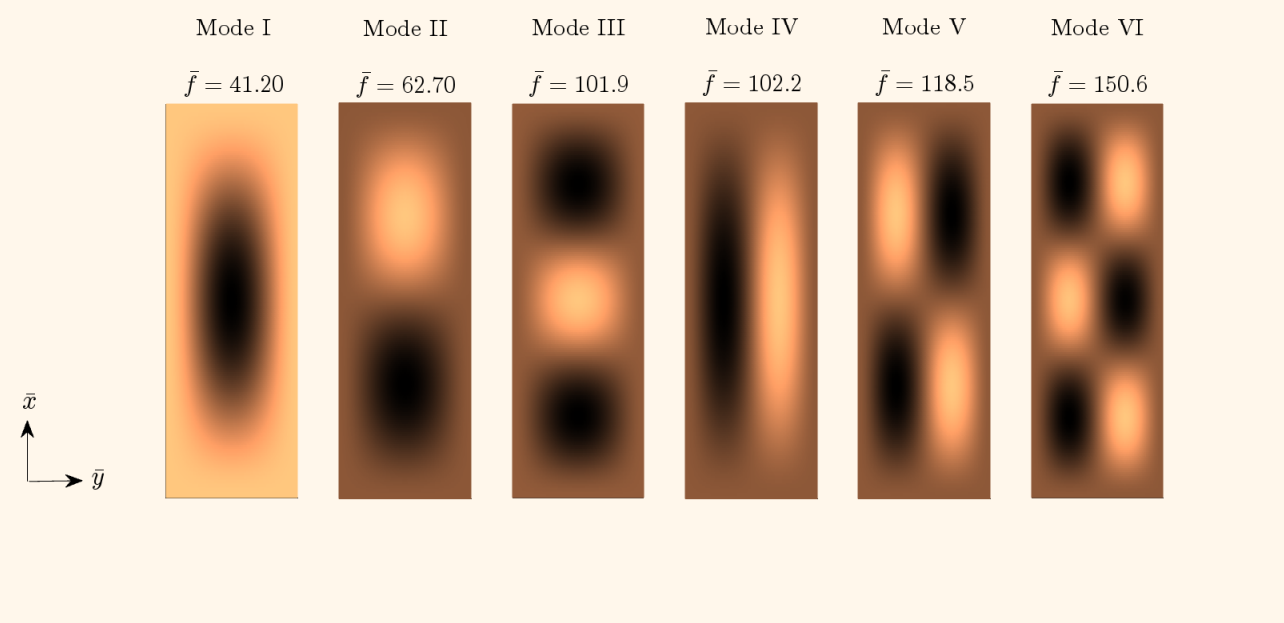

Figure 3: Nondimensional baseline modal shapes and frequencies. For visualisation purposes, the x axis is vertical in the figure. The frequencies are computed to their converged value up the fourth significant digit, as given. Note that the baseline mode shapes are identified through a Roman numeral.

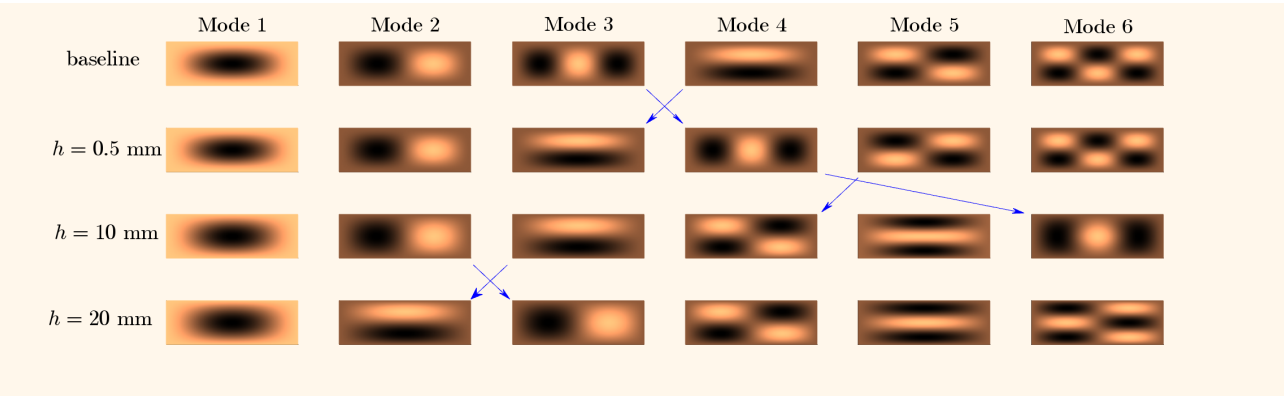

Figure 4: First six mode shapes of Plate 4 under various thickness choices h. Blue lines identify modal crossings.

4. RESULTS AND DISCUSSION

The non-dimensional model is now checked through various numerical experiments. First, the existence of the baseline modal sequence is checked. The smallest thickness ($h = 0.1$ mm) from Table 1 is selected to compute the baseline. The output shapes are scaled frequencies $\bar{f} := \bar{\omega}/2\pi$ are presented in Figure 3. The shapes appear in the same sequence for all four plates, and the scaled frequencies are the same, up to four significant digits, indicating that a common baseline of modal shapes and frequencies exists, as predicted. Since these shapes and frequencies form an invariant set, they will be labelled using Roman numerals: I, II, etc. Further significant digits of precision may be obtained by using smaller meshes, but it is unnecessary for the present purpose. When the thickness is increased, deviations from the baseline appear. Figure 4 shows the evolution of the first six modal shapes for Plate 4 (presenting the smallest surface area across all plates). Modal crossings appear, as well as light distortion of the modal shapes. To assess these differences, Figure 5 presents the MAC for each pair of modes ranging from mode 1 to 6 for all four plates. As can be seen, values close to 1 are always reached for Plate 1. Besides, it is worth noticing how

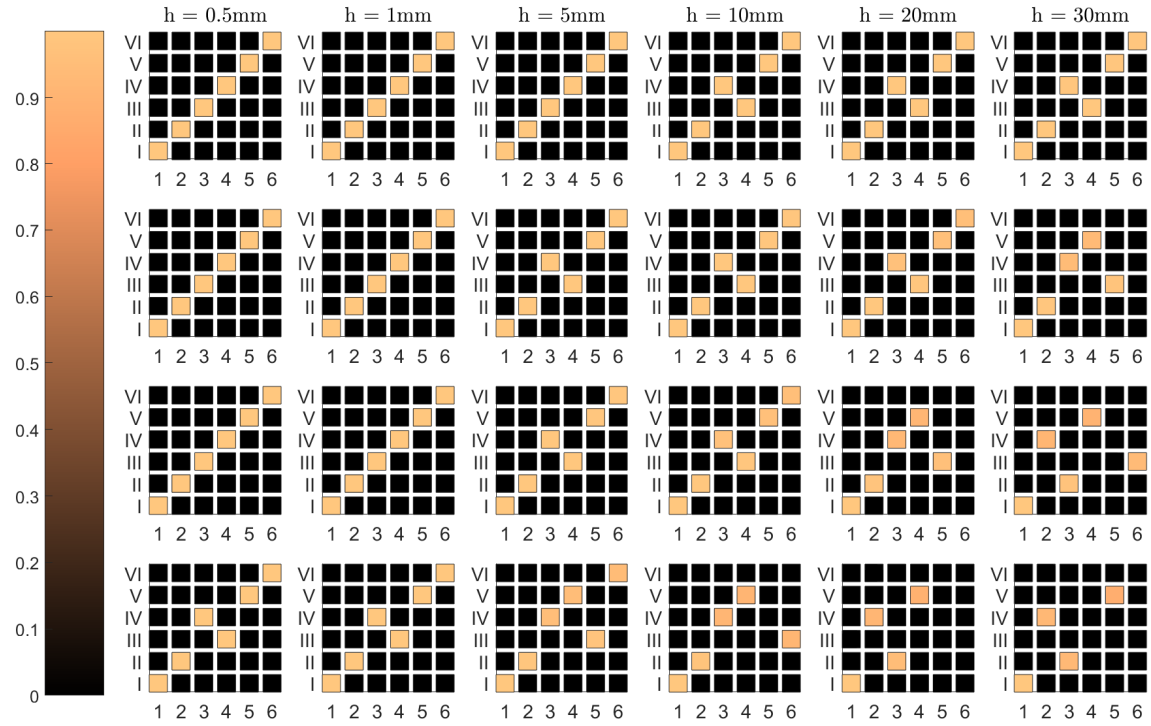

Figure 5: The MAC comparison to the reference plate thickness. From top to bottom: plate 1, plate 2, plate 3, plate 4.

modal crossings for this plate only occur between modes 3 and 4 when considering values of h ≥ 10 mm. On the other hand, a lower correlation is found when the surface area of the plate is decreased. This is already noticeable from Plate 2, for which, despite good correlation indexes reported up to $h = 20$ mm, no correlation is found for the 6^{th} mode at $h = 30$ mm, meaning that only five mode shapes from the reference baseline can be correctly identified within this specific set of modal vectors. Specifically, the corresponding 6^{th} modal shape is here shifted higher up in the modal sequence, hence is not present within the compared set. This kind of deviation is even more frequently noticeable when further reducing the plate's surface area. Accordingly, the lowest correlation is observed for Plate 4. Here, while mode crossing can already be observed at $h = 0.5$ mm, lower correlation values are found for larger h. Finally, a null relationship with the initial baseline is noted for two of the six compared modal shapes for $h = 20$ mm and $h = 30$ mm. A non-dimensional eigenfrequency analysis is available in Figure 6, where discrepancies are reported in cents, that is:

$$\Delta_{cent}\bar{f} := 1200\log_2(\bar{f}_{baseline}/\bar{f}). \tag{17}$$

Here, to compare the correct non-dimensional modal frequencies, the order of the first six eigenshapes at each increased h value was adjusted in accordance with the reference set. Again, this analysis highlights the fact that plates characterized by smaller surface areas tend to diverge at lower h values from the reference set of non-dimensional eigenfrequencies. Overall, as it can be seen, while the lowest differences are observed for Plate 1, the largest deviations appear for the smaller surface area (i.e. Plate 4). In detail, by taking as an example Mode I, no difference is observed up to $h = 1$mm while variations less than 2 cents can still be appreciated up to $h = 5$mm for the same plate. On the other hand, differences higher than 2 cents already emerge at $h = 1$mm and $h = 0.5$mm for Mode I in Plates 3 and 4, respectively.

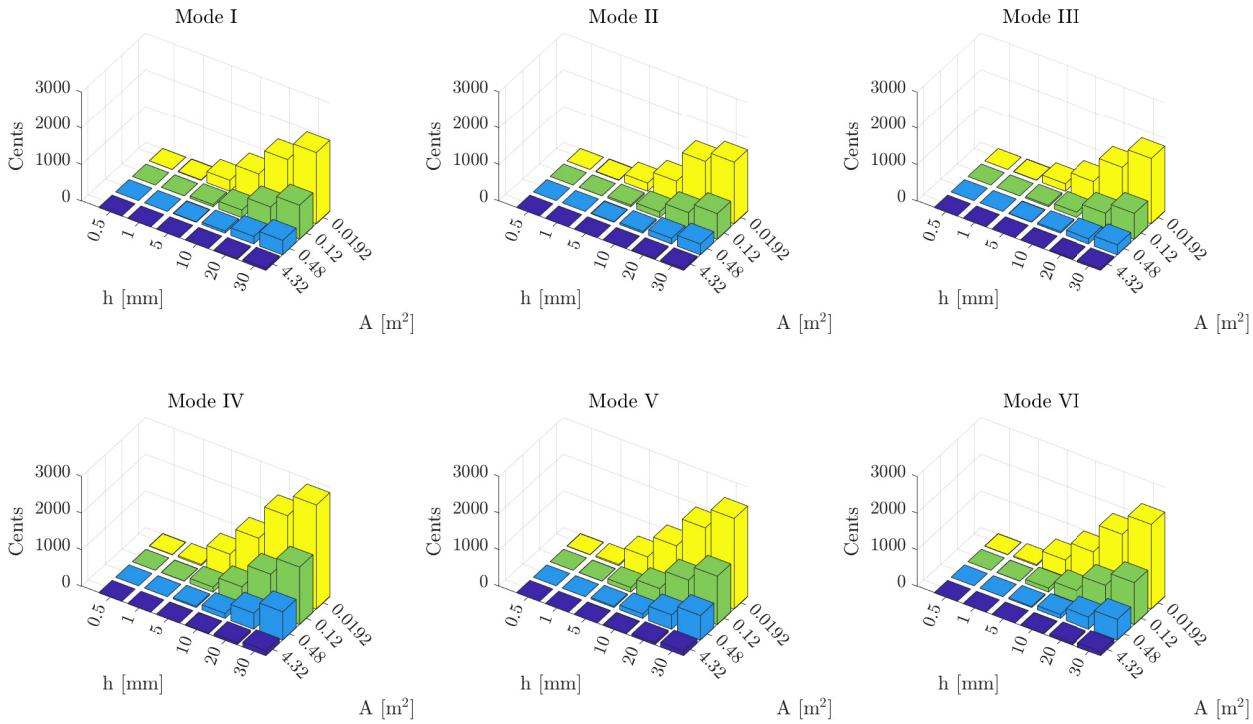

Figure 6: Deviation of the non-dimensional eigenfrequencies from the reference thickness in cents among Plates 1 ($A = 4.32\ m^2$), 2 ($A = 0.48\ m^2$), 3 ($A = 0.12\ m^2$), and 4 ($A = 0.0192\ m^2$) with increasing thickness.

4.1. Scaling laws in the modal domain

The analysis above reveals that deviations from the baseline occur more or less rapidly depending on the plate size. It is useful to plot the deviation of each plate's modal frequencies for the reference mode shapes I-VI. This is done in Figure 7. The deviations are absolute, that is:

$$\Delta\bar{f} := \bar{f}_{baseline} - \bar{f}. \tag{18}$$

When plotted against the thickness, the deviations seem to follow a power law, such that $\Delta\bar{f} \approx$

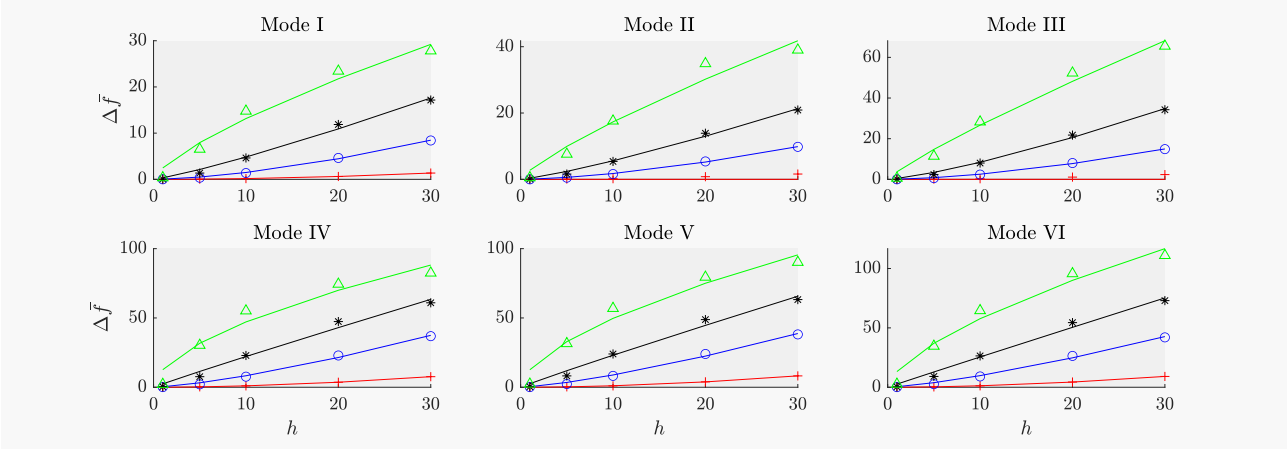

Figure 7: Non-dimensional frequency deviation as a function of h, for the six reference modes. In all plots, the four lines represent the four plates. Colour code: red (Plate 1); blue (Plate 2); black (Plate 3); green (Plate 4). The fits are obtained as $\Delta\bar{f} = ah^b$.

ah^b, where a, b can be found through a fitting procedure. The solid lines in the figure report the

	Mode I	Mode II	Mode III	Mode IV	Mode V	Mode VI
Plate 1	1.9	1.8	1.9	1.8	1.9	1.8
Plate 2	1.6	1.6	1.6	1.4	1.3	1.3
Plate 3	1.2	1.2	1.3	0.96	0.95	0.99
Plate 4	0.73	0.8	0.86	0.57	0.59	0.64

Table 3: Best fit exponents for the curves in Figure 7. Here, the fitting law is as $\Delta\bar{f} = ah^b$.

behaviour of such best fits. Table 3 reports the values of the computed exponents as a function of the plate and modal numbers. A tendency exists leading from quadratic behaviour to square root as the plate area is decreased. The exponent values are somewhat consistent across all six modes for the four plates, indicating some kind of robustness of these results. This is interesting, but it does not help assess the thin-plate behaviour, nor characterise plates sharing the same baseline modal sequence.

In other words, it is not the behaviour of a given plate one is after but a more general feature common to all plates belonging to the same group. In the literature, the use of non-dimensional parameters has been suggested to characterise thin-plate behaviour, such as η as defined in Eq. 13. Note that the surface area and the thickness are natural scaling parameters when the material properties are kept constant, as evidenced by the analysis in Section 2. When plotted against η, the modal frequency deviations appear to collapse to one single curve for each mode, as seen in Figure 8. The fit in this case follows the power law $\Delta\bar{f} = \alpha\eta^{\beta}$, where α, β are non-dimensional parameters. This result is significant because it defines an invariant behaviour for the modal frequency deviations of all the plates sharing the same modal frequency baseline. Also in Figure 8 are the best-fit results obtained in the recommended range for η, as per Eq. 14. In this case, the results for the exponents β are given in Table 4: note that the exponents indicate quasi-linear behaviour. From the figure, a slope change is evident for values of η below 8, indicating the passage to thick-plate behaviour. In other words, the linearity of the modal frequency deviation from the baseline could be used to define thin-plate behaviour in the modal domain, although this claim warrants further investigation.

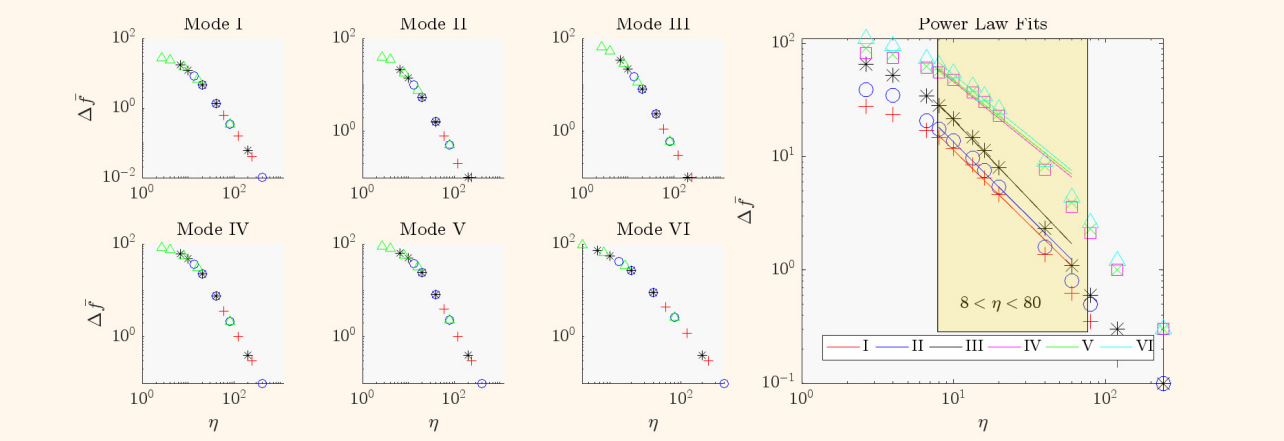

Figure 8: Non-dimensional frequency deviation as a function of the length-to-thickness paramter η as per Eq. 13, for the six reference modes. The plot on the right represents the cumulative power law fit for the six modes in the suggested range as per Eq. 14.

	Mode I	Mode II	Mode III	Mode IV	Mode V	Mode IV
β	-1.3	-1.3	-1.4	-1.1	-1.1	-1.1

Table 4: Best fit results for the scaled modal frequency deviations. Here, $\Delta\bar{f} = \alpha\eta^{\beta}$. The fit was performed on the suggested range for η, as per Eq. 14. Note that the exponents are all quasi-linear, indicating a way of assessing thin-plate behaviour in the modal domain.

5. FINAL COMMENTS AND CONCLUSIONS

This paper introduced a method for assessing the validity of thin-plate assumptions concerning orthotropic boards. The approach relies on eigenshape analysis and comparisons of non-dimensional eigenfrequencies. In contrast to dispersion relation-based analysis on unbounded domains, this approach enables an investigation of discrepancies in thin-model assumptions for a family of plates in the modal domain.

The methodology begins with computing a baseline set of modal shapes and dimensionless eigenfrequencies common to plates sharing the same aspect ratio, boundary conditions and elastic constant ratios. A two-step analysis follows to evaluate the thin plate assumptions. Firstly, a comparison of eigenshapes with the baseline modal set is conducted using modal analysis metrics, such as the Modal Assurance Criterion (MAC), to detect deviations in modal vectors at larger thicknesses. Secondly, a non-dimensional comparison is performed to identify significant frequency deviations in scaled eigenfrequencies at increased thickness intervals. The study demonstrates that:

- Orthotropic plates with the same aspect ratio exhibit identical mode shapes, modal sequence, and non-dimensional eigenfrequencies under thin-plate assumptions.
- Larger deviations in non-dimensional eigenfrequencies occur for smaller length-to-thickness values.
- A quasi-linear relationship is observed between deviations in non-dimensional frequencies and the length-to-thickness parameter under thin plate assumptions.

Plate 3 in the study serves as a case study to illustrate the applicability of the described methodology. This plate shares dimensions with a typical guitar half-board, commonly thinned to approximately 3 mm for guitar-making purposes. Analysis reveals that Plate 3 starts exhibiting modal crossing and larger deviations in non-dimensional eigenfrequencies (> 7 cents) only at $h \geq 5$ mm, indicating good agreement with thin plate model assumptions up to 5 mm. This assumption aligns with previous research on guitar plate modelling. These findings confirm the applicability of the introduced comparative analysis for studying orthotropic plates.

ACKNOWLEDGEMENTS

This work received funding from the European Research Council (ERC) under the Horizon2020 framework, grant number 950084 - StG - NEMUS.

REFERENCES

1. N.H. Fletcher and T. D. Rossing. *The physics of musical instruments.* Springer Science & Business Media, New York, 2012.
2. K. Ege. *La table d'harmonie du piano – Études modales en basses et moyennes fréquences.* PhD thesis, 'École Polytechnique, Paris, France, 2009.
3. K.F. Graff. *Wave Motion in Elastic Solids.* Dover Publications, New York, 1991.

4. MJ. Elejabarrieta, A. Ezcurra, and C. Santamaría. Vibrational behaviour of the guitar soundboard analysed by the finite element method. *Acta Acustica united with Acustica*, 87(1):128–136, 2001.
5. G. Derveaux, A. Chaigne, P. Joly, and E. Bécache. Time-domain simulation of a guitar: Model and method. *The Journal of the Acoustical Society of America*, 114(6):3368–3383, 2003.
6. Y. Giro, J-L. Le Carrou, A. Vincenti, S. Dartois, R. Viala, and B. Navarret. Predicting the effects of bracing pattern modifications on acoustic guitar soundboards. In *Forum Acusticum*, pages 3419–3422, Turin, Italy, September 2023.
7. C. E. Gough. A violin shell model: Vibrational modes and acoustics. *The Journal of the Acoustical Society of America*, 137(3):1210–1225, 2015.
8. A. Santoni, S. Schoenwald, B. Van Damme, and P. Fausti. Determination of the elastic and stiffness characteristics of cross-laminated timber plates from flexural wave velocity measurements. *Journal of Sound and Vibration*, 400:387–401, 2017.
9. T. Krauthammer and E. Ventsel. *Thin plates and shells: theory, analysis and applications*. Mercel Dekker Inc., New York, 2001.
10. V. Bucur. *Handbook of materials for string musical instruments*. Springer, Cham, Switzerland, 2016.
11. M. Ducceschi and S. Bilbao. Linear stiff string vibrations in musical acoustics: Assessment and comparison of models. *The Journal of the Acoustical Society of America*, 140(4):2445–2454, 2016.
12. M. Ducceschi and S. Bilbao. Conservative finite difference time domain schemes for the prestressed Timoshenko, shear and Euler-Bernoulli beam equations. *Wave Motion*, 89:142 – 165, 2019.
13. M. Ducceschi, S. Duran, H. Tahvanainen, and L. Ausiello. A method to estimate the rectangular orthotropic plate elastic constants using least-squares and chladni patterns. *Applied Acoustics*, 220:109949, 2024.
14. P. Avitabile. *Modal testing: A practitioner's guide*. John Wiley & Sons, Hoboken, New Jersey, 2017.